Multi-wavelength observations of Active Galactic Nuclei in the Fornax Cluster.

Dejene Zewdie[1], **and S Ilani Loubser**[1]

[1]Centre for Space Research, North-West University, Potchefstroom 2520, South Africa

E-mail: dzewdie@gmail.com.

Abstract. We report a multiwavelength study of active galactic nuclei (AGNs) in the Fornax cluster using X-rays data from eROSITA, optical spectroscopic observations from MUSE, and infrared imaging from WISE. The recently reported X-ray luminosity of Fornax cluster members of FCC121 and FCC179, identifies them as AGN. We also estimate that the X-ray luminosity of FCC184 is not reported; however, it is detected in the X-ray luminosity, and we estimate the X-ray luminosity. Using optical emission lines, we classify the photoionisation mechanism as classified those galaxies in different populations of FCC179 as star-forming galaxy, FCC121 are classified as composite galaxy, and FCC184 is classified as low-ionisation nuclear emission-line region (LINER). Even through X-ray observation, we found that FCC184 has a luminosity of 0.2 to 2.3 keV which is $\log \mathrm{Lx} = 40.39\ \mathrm{erg\ s^{-1}}$, but its infrared properties are not typical of an AGN. Neutral hydrogen is detected in these three galaxies. Interestingly, FCC179 the HI morphology could be from AGN feedback. These multiwavelength observations reveal different types of AGN populations that play an important role in the cluster environment.

1 Introduction

Active galactic nuclei (AGN) are energetic objects that are powered by the accretion of matter onto a supermassive black hole (SMBH) in the central regions of the galaxy. These objects can generate a significant amount of radiative energy across the electromagnetic spectrum. According to the unified model [1] and based on their physical properties, AGNs are broadly classified according to the line of sight of the observers to the accretion disk. This central region is surrounded by a toroidal structure of dust and gas, which can lead to vastly different appearances when observed from different viewing angles. Depending on how much dust is found along the line of sight, AGNs can be classified into two main types: Type 1 AGN and Type 2 AGN. Type 1 AGNs (unobscured) are those in those where we have a direct line of sight towards the central engine, while Type 2 AGNs (obscured) are those where dusty clouds block our view of the accretion disk and the broad-line region.

Massive galaxies are believed to have a SMBH with a mass in excess of $\geq 10^6 \mathrm{M}\odot$ at the centre; however, in most cases the SMBH is inactive [2]. SMBHs accrete most of their mass through AGN activity [3] and mergers. AGN activity in merging galaxies is obscured, both by dust in the optical and UV wavelengths, and by atomic gas in the X-ray regime. Numerical models [4] suggest that AGN activity plays an important role in quenching star formation in massive galaxies through a process referred to as AGN feedback, in which the energy released from the AGN (either radiatively or mechanically through jets) heats and removes the cold gas reservoirs. However, major mergers trigger intense episodes of star formation and obscured AGN activity [4]. With the complex nature of AGN, multiwavelength observations are crucial to gaining a better understanding of the physics of AGN structure, formation, and evolution and their role in the host galaxy.

The Fornax cluster, one of the closest clusters in the Southern Hemisphere, is actively assembling mass, and with dense physical processes [5]. Several multi-wavelength observing campaigns were conducted to better understand the cluster environment and the mechanisms driving galaxy transformation. These include deep-optical

imaging from the Fornax Deep Survey (FDS) [6, 7], which aimed to explore the structure and evolution of low-surface brightness features of dwarf galaxies. The MeerKAT Fornax Survey, which focusses on neutral hydrogen (HI) maps, and to trace the gas content in the galaxy [8, 9]. The Fornax3D survey [10], uses deep integral field spectroscopic observations for 33 bright galaxies within the virial radius of the Fornax cluster and provided detailed internal kinematics, dynamical structures, and evolutionary histories within the cluster. In the Fornax cluster there are different types of galaxies that provide a unique laboratory for understanding the role of AGNs in dense environments.

Recently, eROSITA observation of the Virgo and Fornax clusters shows that the detected X-ray sources are 50 and 10, respectively, and the X-ray AGN occupation rate is 3% in both clusters [11], which is less than in the field. In the Fornax cluster, 10 galaxies are detected by soft X-ray, and only one of them, FCC121, is detected by hard X-ray with a 2.3-5 keV luminosity of $6.6 \times 10^{41} \mathrm{ergs}^{-1}$ [11].

In this paper, we used two AGN selection techniques to confirm sources detected by X-rays in the Fornax cluster, which should allow an understanding of the role of AGN in the cluster environment. This paper is arranged as follows. In Section 2, we describe the available multiwavelength observations. In Section 3, we describe the results and discussion of the multi-wavelength observations and AGN classified in the Fornax galaxies. In Section 4, we summarise the main findings of this work. Throughout this paper, we assume a standard ΛCDM cosmology with $\mathrm{H}_0 = 70\ \mathrm{km\ s^{-1}\ pc^{-1}}$, $\Omega_\Lambda = 0.7$, and $\Omega_M = 0.3$, and all magnitudes present in the AB system and the wide-field infrared survey Explorer (WISE) Vega system.

2 Multi-Wavelength Observations

In this study, we used publicly available data from the Spectrum-Roentgen-Gamma/eROSITA all-sky survey, optical spectroscopic data from Multi-Unit Spectroscopic Explorer (MUSE), and infrared data from WISE imaging. These three multi-wavelength observed galaxies are FCC121, FCC179, and FCC184. These galaxies are gas-rich, neutral hydrogen detected with MeerKAT, the detailed analysis of ionised gas properties for those galaxies found in Zewdie et al. (in preparation).

2.1 eROSITA X-ray Data

We used a publicly available X-ray detected source catalogue [12] from the eROSITA all-sky survey [13]. The survey includes a soft band (0.2 to 2.3 keV) and a hard band (2.3 to 5 keV). Recently, Hou et al. [11] studied the X-ray detected AGNs in the nearest two clusters, namely Virgo and Fornax. They used a 10 arcsec radius to cross-match for both clusters, which corresponds to the physical scale of 0.8 kpc and 1.0 kpc, respectively. We repeated their experiment and found FCC184 with a 9.56 arcsec separation distance, which is 0.86 kpc. Therefore, we also estimate the X-ray luminosity of FC184 and find that at 0.2 to 2.3 keV it is $\log \mathrm{Lx} = 40.39\ \mathrm{erg\ s^{-1}}$ and the X-ray luminosity of FCC121 and FCC179 is 41.31 and 40.23 $\mathrm{erg\ s^{-1}}$, respectively [11].

2.2 MUSE Optical Spectroscopy data

The VLT/MUSE offers a field of view (FoV) of 1×1 arcmin^2, with a spatial sampling of 0.2×0.2 arcsec^2 per pixel. It covers a wavelength range of 4560 to 9300 Å, with a spectral sampling of 1.25 Å per pixel and a spectral resolution of ~ 2.5 Å [14]. A large number of galaxies in the Fornax cluster were targeted within the MUSE observations with the Fornax3D survey [10], which targeted galaxies brighter than $\mu_\mathrm{B} = 15\ \mathrm{mag}$ in order to provide spatially resolved spectroscopy. We extracted nuclear spectra from the centre using 2 arcsec apertures and fit Gaussian profiles for Hα, [NII], [OIII], and Hβ wavelengths. We used these four optical emission lines to classify galaxies according to their photo-ionisation mechanism using the Baldwin, Phillips & Terlevich (BPT) diagram [15]. With this BPT classification, we can classify galaxies as star-forming, AGN (Seyfert or LINER), or composite regions of both star-forming and AGNs.

2.3 WISE data

The WISE mission observed the full sky in four mid-IR photometric bands, centred at 3.4, 4.6, 12, and 22 μm (named W1, W2, W3, and W4), respectively. We used WISE colours to investigate the existence of IR-obscured AGN activity in the Fornax cluster. We used the colour cut for WISE AGN, $\mathrm{W1} - \mathrm{W2} > 0.7$ mag, and provided a sample with 90 percent reliability [16].

3 Results and Discussion

3.1 Multiwavelength observations of AGNs in the Fornax cluster

The Fornax cluster is targeted with different instruments, all archival observations, mostly from all-sky surveys. We emphasise that each wavelength probed gives a better understanding of different types of AGN populations. We are interested in sources detected by X-rays in the Fornax cluster [11]; however, only two of these sources have

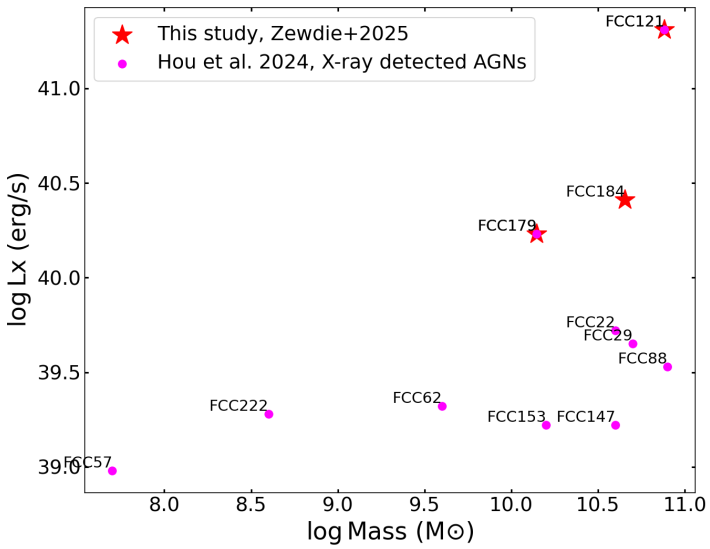

Figure 1: All soft X-ray detected galaxies in the Fornax cluster. The magenta dots are reported by Hou et al. [11] and the red star are our targets. FCC121 is hard X-ray detected. However, FCC184 was not reported as X-ray detected by Hou et al. [11], we estimated the X-ray luminosity and found that it to be the range of the X-ray luminosities reported in the Fornax cluster.

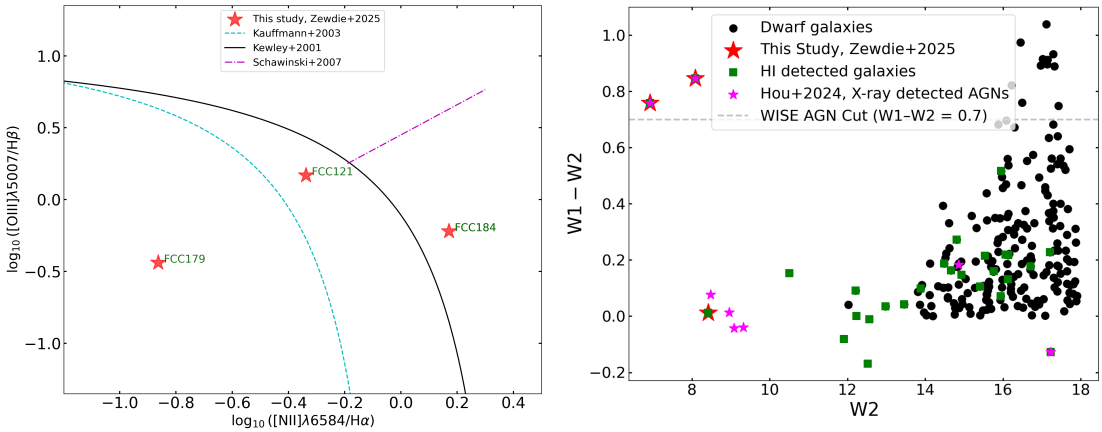

Figure 2: (*left*) The BPT diagram for the three multiwavelength observed galaxies (red stars) in the Fornax cluster. FCC121, FCC179 and FCC184 are classified as composite Star-forming galaxies and a LINER, respectively. The dashed line shows the [17] separation between pure star-forming and composite galaxies (mix of starburst and AGNs). The solid line represents the Kewley et al. [18] division between composite galaxies and AGN dominant and the dashed-dotted line shows the separation between Seyfert 2 and LINER sources [19]. (*right*) The horizontal dashed line is the WISE AGN cur, W1-W2>0.7 [16]. The green square are HI detected galaxies with MeerKAT [20], the magenta star are X-ray detected AGN candidates [11], the black dots are Fornax member galaxies from FDS [21] and the red star are the three the targets.

optical spectroscopic observations. We also found one X-ray-detected source, FCC184, which was not previously reported as X-ray-detected sources. All galaxies are also detected with MeerKAT. Figure 1 shows the 10 soft X-

ray sources [11] including FCC184. All soft X-ray luminosities are ≥ 39 ergs^{-1}, indicating the dominance of a genuine X-ray AGN that has X-ray detection.

As shown in Figure 2, FCC179 can be classified as X-ray detected galaxies; however, with BPT it is a star-forming galaxy, and this might be the ionisation radiation could be obscued or diluted by tourus. Interestingly, FCC121 is classified as a composite galaxy; however, this galaxy is detected in both soft and hard X-ray bands and WISE colour selection can clearly be classified as an AGN. Hou et al. As can be seen in Figure2, all X-ray-detected sources [11] also detected in WISE, however, it does not classify them as AGNs. We also looked at those galaxies with optical spectroscopic observations and three of them are observed by MUSE and the WISE classification as shown in Figure 2, FCC121 and FCC179 are classified. FCC184 is classified, according to the BPT, as a low luminosity AGN. However, this galaxy in the WISE W1 and W2 mag is quite similar, which leads to this galaxy not being classified as an AGN by WISE.

Figure 3 shows the Ha map with the HI column density overplotted. The strong Ha emission in the centre is likely coming from AGN for each of the galaxies. The figures for FCC121 and FCC179 clearly show the HI gas distribution and, in particular, the HI gas in FCC179 seems to be the HI gas pushed away by the AGN central HI,likely by AGN feedback clearing gas.

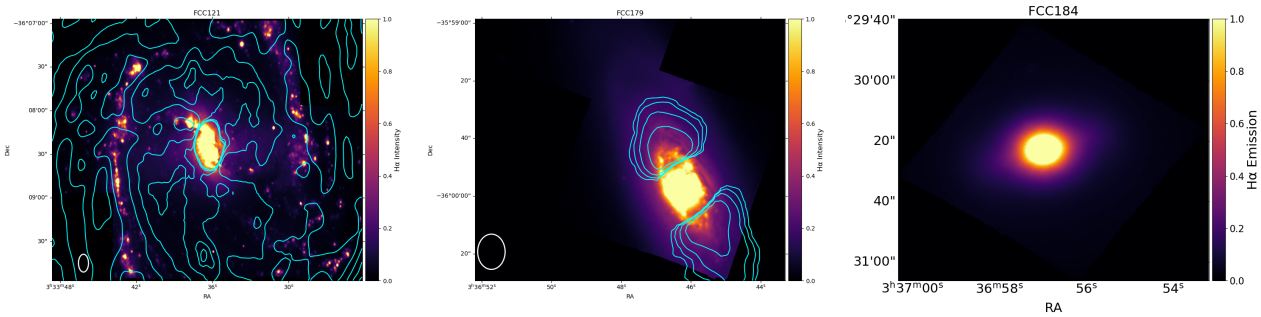

Figure 3: The Hα emission maps for the three galaxies that we highlight in this paper. MUSE observed and HI-detected sources. The Left (FCC121) and meddle (FCC179) panel are the HI detected resolved clearly, and the FCC184 (right-panel) the HI not resolved.

4 Conclusions

We used a recently published released X-ray source catalogue from eROSITA to identify X-ray-detected galaxies in the Fornax cluster. Then we looked at archival data from MUSE and WISE to supplement the radio and X-ray observations. We found three X-ray-detected sources observed with MUSE, WISE, and MeerKAT and discuss their details here. From these three galaxies, FCC121 is the only one classified as an AGN with all the selection criteria investigated here. FCC179 is classified as a WISE AGN; however, the BPT classification classifies it as a star-forming galaxy. This suggests that the galaxy could be heavily obscured by dust. Interestingly, the HI gas morphology can show feedback and likely shows AGN pushing gas away. From our multi-wavelength observations data, the X-ray luminosity of FCC184 is quite similar to the X-ray luminosity of FCC179, and classifies as AGN with BPT, whereas the WISE data does not. These LINER-like emission could be produced by stellar mechanisms, such as hot post-AGB stars. This study shows that sources are classified differently by classification schemes in different wavelengths and highlights the need to study sources with multi-wavelength data.

5 Aknowledgements

This work is based on research supported in part by the National Research Foundation (NRF) of South Africa (NRF Grant Number: CPRR240414214079). Any opinion, finding, and conclusion or recommendation expressed in this material is that of the author(s), and the NRF does not accept any liability in this regard.

References

[1] R. Antonucci, "Unified models for active galactic nuclei and quasars." *ARA&A*, vol. 31, pp. 473–521, Jan. 1993.

[2] P. Padovani, D. M. Alexander, R. J. Assef, B. De Marco, P. Giommi, R. C. Hickox, G. T. Richards, V. Smolcic, E. Hatziminaoglou, V. Mainieri, and M. Salvato, "Active galactic nuclei: what's in a name?" *A&A Rev.*, vol. 25, no. 1, p. 2, Aug. 2017.

[3] A. Soltan, "Masses of quasars." *MNRAS*, vol. 200, pp. 115–122, Jul. 1982.

[4] P. F. Hopkins, L. Hernquist, T. J. Cox, and D. Kereš, "A Cosmological Framework for the Co-Evolution of Quasars, Supermassive Black Holes, and Elliptical Galaxies. I. Galaxy Mergers and Quasar Activity," *ApJS*, vol. 175, no. 2, pp. 356–389, Apr. 2008.

[5] M. J. Drinkwater, M. D. Gregg, and M. Colless, "Substructure and Dynamics of the Fornax Cluster," *ApJ*, vol. 548, no. 2, pp. L139–L142, Feb. 2001.

[6] E. Iodice, M. Capaccioli, A. Grado, L. Limatola, M. Spavone, N. R. Napolitano, M. Paolillo, R. F. Peletier, M. Cantiello, T. Lisker, C. Wittmann, A. Venhola, M. Hilker, R. D'Abrusco, V. Pota, and P. Schipani, "The Fornax Deep Survey with VST. I. The Extended and Diffuse Stellar Halo of NGC 1399 out to 192 kpc," *ApJ*, vol. 820, no. 1, p. 42, Mar. 2016.

[7] A. Venhola, R. Peletier, E. Laurikainen, H. Salo, E. Iodice, S. Mieske, M. Hilker, C. Wittmann, T. Lisker, M. Paolillo, M. Cantiello, J. Janz, M. Spavone, R. D'Abrusco, G. van de Ven, N. Napolitano, G. Verdoes Kleijn, N. Maddox, M. Capaccioli, A. Grado, E. Valentijn, J. Falcón-Barroso, and L. Limatola, "The Fornax Deep Survey with the VST. IV. A size and magnitude limited catalog of dwarf galaxies in the area of the Fornax cluster," *A&A*, vol. 620, p. A165, Dec. 2018.

[8] P. Serra, W. J. G. de Blok, G. L. Bryan, S. Colafrancesco, R. J. Dettmar, B. S. Frank, F. Govoni, G. I. G. Jozsa, R. C. Kraan-Korteweg, F. M. Maccagni, S. I. Loubser, M. Murgia, T. A. Oosterloo, R. F. Peletier, R. Pizzo, L. Richter, M. Ramatsoku, M. W. L. Smith, S. C. Trager, J. H. van Gorkom, and M. A. W. Verheijen, "The MeerKAT Fornax Survey," in *MeerKAT Science: On the Pathway to the SKA*, Jan. 2016, p. 8.

[9] D. Kleiner, P. Serra, F. M. Maccagni, M. A. Raj, W. J. G. de Blok, G. I. G. Józsa, P. Kamphuis, R. Kraan-Korteweg, F. Loi, A. Loni, S. I. Loubser, D. C. Molnár, T. A. Oosterloo, R. Peletier, and D. J. Pisano, "The MeerKAT Fornax Survey. II. The rapid removal of H I from dwarf galaxies in the Fornax cluster," *A&A*, vol. 675, p. A108, Jul. 2023.

[10] M. Sarzi, E. Iodice, L. Coccato, E. M. Corsini, P. T. de Zeeuw, J. Falcón-Barroso, D. A. Gadotti, M. Lyubenova, R. M. McDermid, G. van de Ven, K. Fahrion, A. Pizzella, and L. Zhu, "Fornax3D project: Overall goals, galaxy sample, MUSE data analysis, and initial results," *A&A*, vol. 616, p. A121, Aug. 2018.

[11] M. Hou, Z. Hu, and Z. Li, "An X-Ray Census of Active Galactic Nuclei in the Virgo and Fornax Clusters of Galaxies with SRG/eROSITA," *ApJ*, vol. 965, no. 2, p. L24, Apr. 2024.

[12] A. Merloni, G. Lamer, T. Liu, M. E. Ramos-Ceja, H. Brunner, E. Bulbul, K. Dennerl, V. Doroshenko, M. J. Freyberg, S. Friedrich, E. Gatuzz, A. Georgakakis, F. Haberl, Z. Igo, I. Kreykenbohm, A. Liu, C. Maitra, A. Malyali, M. G. F. Mayer, K. Nandra, P. Predehl, J. Robrade, M. Salvato, J. S. Sanders, I. Stewart, D. Tubín-Arenas, P. Weber, J. Wilms, R. Arcodia, E. Artis, J. Aschersleben, A. Avakyan, C. Aydar, Y. E. Bahar, F. Balzer, W. Becker, K. Berger, T. Boller, W. Bornemann, M. Brüggen, M. Brusa, J. Buchner, V. Burwitz, F. Camilloni, N. Clerc, J. Comparat, D. Coutinho, S. Czesla, S. M. Dannhauer, L. Dauner, T. Dauser, J. Dietl, K. Dolag, T. Dwelly, K. Egg, E. Ehl, S. Freund, P. Friedrich, R. Gaida, C. Garrel, V. Ghirardini, A. Gokus, G. Grünwald, S. Grandis, I. Grotova, D. Gruen, A. Gueguen, S. Hämmerich, N. Hamaus, G. Hasinger, K. Haubner, D. Homan, J. Ider Chitham, W. M. Joseph, A. Joyce, O. König, D. M. Kaltenbrunner, A. Khokhriakova, W. Kink, C. Kirsch, M. Kluge, J. Knies, S. Krippendorf, M. Krumpe, J. Kurpas, P. Li, Z. Liu, N. Locatelli, M. Lorenz, S. Müller, E. Magaudda, C. Mannes, H. McCall, N. Meidinger, M. Michailidis, K. Migkas, D. Muñoz-Giraldo, B. Musiimenta, N. T. Nguyen-Dang, Q. Ni, A. Olechowska, N. Ota, F. Pacaud, T. Pasini, E. Perinati, A. M. Pires, C. Pommranz, G. Ponti, K. Poppenhaeger, G. Pühlhofer, A. Rau, M. Reh, T. H. Reiprich, W. Roster, S. Saeedi, A. Santangelo, M. Sasaki, J. Schmitt, P. C. Schneider, T. Schrabback, N. Schuster, A. Schwope, R. Seppi, M. M. Serim, S. Shreeram, E. Sokolova-Lapa, H. Starck, B. Stelzer, J. Stierhof, V. Suleimanov, C. Tenzer, I. Traulsen, J. Trümper, K. Tsuge, T. Urrutia, A. Veronica, S. G. H. Waddell, R. Willer, J. Wolf, M. C. H. Yeung, A. Zainab, F. Zangrandi, X. Zhang, Y. Zhang, and X. Zheng, "The SRG/eROSITA all-sky survey. First X-ray catalogues and data release of the western Galactic hemisphere," *A&A*, vol. 682, p. A34, Feb. 2024.

[13] R. Sunyaev, V. Arefiev, V. Babyshkin, A. Bogomolov, K. Borisov, M. Buntov, H. Brunner, R. Burenin, E. Churazov, D. Coutinho, J. Eder, N. Eismont, M. Freyberg, M. Gilfanov, P. Gureyev, G. Hasinger, I. Khabibullin, V. Kolmykov, S. Komovkin, R. Krivonos, I. Lapshov, V. Levin, I. Lomakin, A. Lutovinov, P. Medvedev, A. Merloni, T. Mernik, E. Mikhailov, V. Molodtsov, P. Mzhelsky, S. Müller, K. Nandra, V. Nazarov, M. Pavlinsky, A. Poghodin, P. Predehl, J. Robrade, S. Sazonov, H. Scheuerle, A. Shirshakov, A. Tkachenko, and V. Voron, "SRG X-ray orbital observatory. Its telescopes and first scientific results," *A&A*, vol. 656, p. A132, Dec. 2021.

[14] R. Bacon, M. Accardo, L. Adjali, H. Anwand, S. Bauer, I. Biswas, J. Blaizot, D. Boudon, S. Brau-Nogue, J. Brinchmann, P. Caillier, L. Capoani, C. M. Carollo, T. Contini, P. Couderc, E. Daguisé, S. Deiries, B. Delabre, S. Dreizler, J. Dubois, M. Dupieux, C. Dupuy, E. Emsellem, T. Fechner, A. Fleischmann, M. François, G. Gallou, T. Gharsa, A. Glindemann, D. Gojak, B. Guiderdoni, G. Hansali, T. Hahn, A. Jarno, A. Kelz, C. Koehler, J. Kosmalski, F. Laurent, M. Le Floch, S. J. Lilly, J. L. Lizon, M. Loupias, A. Manescau, C. Monstein, H. Nicklas, J. C. Olaya, L. Pares, L. Pasquini, A. Pécontal-Rousset, R. Pelló, C. Petit, E. Popow, R. Reiss, A. Remillieux, E. Renault, M. Roth, G. Rupprecht, D. Serre, J. Schaye, G. Soucail, M. Steinmetz, O. Streicher, R. Stuik, H. Valentin, J. Vernet, P. Weilbacher, L. Wisotzki, and N. Yerle, "The MUSE second-generation VLT instrument," in *Ground-based and Airborne Instrumentation for Astronomy III*, ser. Society of Photo-Optical Instrumentation Engineers (SPIE) Conference Series, I. S. McLean, S. K. Ramsay, and H. Takami, Eds., vol. 7735, Jul. 2010, p. 773508.

[15] J. A. Baldwin, M. M. Phillips, and R. Terlevich, "Classification parameters for the emission-line spectra of extragalactic objects." *PASP*, vol. 93, pp. 5–19, Feb. 1981.

[16] R. J. Assef, D. Stern, C. S. Kochanek, A. W. Blain, M. Brodwin, M. J. I. Brown, E. Donoso, P. R. M. Eisenhardt, B. T. Jannuzi, T. H. Jarrett, S. A. Stanford, C. W. Tsai, J. Wu, and L. Yan, "Mid-infrared Selection of Active Galactic Nuclei with the Wide-field Infrared Survey Explorer. II. Properties of WISE-selected Active Galactic Nuclei in the NDWFS Boötes Field," *ApJ*, vol. 772, no. 1, p. 26, Jul. 2013.

[17] G. Kauffmann, T. M. Heckman, C. Tremonti, J. Brinchmann, S. Charlot, S. D. M. White, S. E. Ridgway, J. Brinkmann, M. Fukugita, P. B. Hall, Ž. Ivezić, G. T. Richards, and D. P. Schneider, "The host galaxies of active galactic nuclei," *MNRAS*, vol. 346, no. 4, pp. 1055–1077, Dec. 2003.

[18] L. J. Kewley, B. Groves, G. Kauffmann, and T. Heckman, "The host galaxies and classification of active galactic nuclei," *MNRAS*, vol. 372, no. 3, pp. 961–976, Nov. 2006.

[19] K. Schawinski, D. Thomas, M. Sarzi, C. Maraston, S. Kaviraj, S.-J. Joo, S. K. Yi, and J. Silk, "Observational evidence for AGN feedback in early-type galaxies," *MNRAS*, vol. 382, no. 4, pp. 1415–1431, Dec. 2007.

[20] D. Kleiner, P. Serra, F. M. Maccagni, A. Venhola, K. Morokuma-Matsui, R. Peletier, E. Iodice, M. A. Raj, W. J. G. de Blok, A. Comrie, G. I. G. Józsa, P. Kamphuis, A. Loni, S. I. Loubser, D. C. Molnár, S. S. Passmoor, M. Ramatsoku, A. Sivitilli, O. Smirnov, K. Thorat, and F. Vitello, "A MeerKAT view of pre-processing in the Fornax A group," *A&A*, vol. 648, p. A32, Apr. 2021.

[21] A. H. Su, H. Salo, J. Janz, A. Venhola, and R. F. Peletier, "Photometric properties of nuclear star clusters and their host galaxies in the Fornax cluster," *A&A*, vol. 664, p. A167, Aug. 2022.